

Resonance Raman Characterization of Different Forms of Ground-State 8-Bromo-7-hydroxyquinoline Caged Acetate in Aqueous Solutions

Hui-Ying An,[†] Chensheng Ma,[†] Jameil L. Nganga,[‡] Yue Zhu,[‡] Timothy M. Dore,^{*,‡} and David Lee Phillips^{*,†}

Department of Chemistry, The University of Hong Kong, Pokfulam Road, Hong Kong S.A.R., P. R. China, and Department of Chemistry, University of Georgia, Athens, Georgia 30602-2556, U.S.A

Received: October 30, 2008; Revised Manuscript Received: January 15, 2009

The 8-bromo-7-hydroxyquinolyl group (BHQ) is a derivative of 7-hydroxyquinoline (7-HQ) and BHQ molecules coexisting as different forms in aqueous solution. Absorption and resonance Raman spectroscopic methods were used to examine 8-bromo-7-hydroxyquinoline protected acetate (BHQ–OAc) in acetonitrile (MeCN), H₂O/MeCN (60:40, v/v, pH 6~7), and NaOH–H₂O/MeCN (60:40, v/v, pH 11~12) to obtain a better characterization of the forms of the ground-state species of BHQ–OAc in aqueous solutions and to examine their properties. The absorption spectra of BHQ–OAc in water show no absorption bands of the tautomeric species unlike the strong band at about 400 nm observed for the tautomeric form in 7-HQ aqueous solution. The resonance Raman spectra in conjunction with Raman spectra predicted from density functional theory (DFT) calculations reveal the observation of a double Raman band system characteristic of the neutral form (the nominal C=C ring stretching, C–N stretching, and O–H bending modes at 1564 and 1607 cm⁻¹) and a single Raman band diagnostic of the enol-deprotonated anionic form (the nominal C=C ring, C–N, and C–O⁻ stretching modes in the 1593 cm⁻¹ region). These results suggest that the neutral form of BHQ–OAc is the major species in neutral aqueous solution. There is a modest increase in the amount of the anionic form and a big decrease in the amount of the tautomeric form of the molecules for BHQ–OAc compared to 7-HQ in neutral aqueous solution. The presence of the 8-bromo group and/or competitive hydrogen bonding that hinder the formation and transfer process of a BHQ–OAc–water cyclic complex may be responsible for this large substituent effect.

Introduction

It is useful to have a range of phototrigger compounds available that selectively release a biologically active substance at specific times and places within a biological system to better investigate the temporal and spatial changes occurring during physiological processes. There has been increasing interest in developing phototriggers that are excited by multiphoton processes to release the biological effectors^{1–3} because this can enable improved control of the excitation volume to about 1 fL, which is noticeably smaller than the size of typical mammalian cells or neurons. Whereas both one-photon excitation (1PE) using UV or near-UV light and multiphoton excitation (MPE) processes like two-photon excitation (2PE) using infrared (IR) light enable excellent control of the timing of the excitation of the phototriggers, MPE methods can significantly improve 3D spatial monitoring,^{2–4} and the use of lower energy IR light minimizes tissue damage, light absorption, and scattering, making deeper penetration into biological samples possible. The use of IR light also facilitates the conduct of longer experiments on living biological systems due to lower amounts of damage compared to the UV or near-UV excitation typically utilized by 1PE of phototriggers.^{2–4}

Phototrigger compounds that have chromophores with enough sensitivity to 2PE that can be employed in physiology experiments are relatively rare, yet phototriggers based on 8-bromo-7-hydroxycoumarin (such as Bhc and Bhc-diol) were observed to have a good sensitivity to 2PE and have been employed as protecting groups for a number of biological effectors.^{3,5} Nevertheless, these Bhc and Bhc-diol phototrigger compounds have relatively low solubility in aqueous buffers of high ionic strength and exhibit a large amount of fluorescence upon excitation that can limit their use in physiology experiments. The 8-bromo-7-hydroxyquinolyl group (BHQ) was found to be efficiently photolyzed by 1PE and 2PE in aqueous buffers at physiological pH with a high quantum efficiency and low levels of fluorescence that make this kind of phototrigger more attractive for utilization in biological experiments.^{6,7} Recent work showed a very fast process of the deprotection and solvolysis of 8-bromo-7-hydroxyquinoline caged acetate (BHQ–OAc) to form the byproduct (BHQ–OH).⁷ These results suggest that it would be useful to employ ultrafast (femtoseconds to picoseconds) and fast (nanoseconds to microseconds) spectroscopic methods to directly follow the photophysics and photochemistry associated with the deprotection and formation of the byproduct to better understand its reaction mechanism (particularly in aqueous environments).

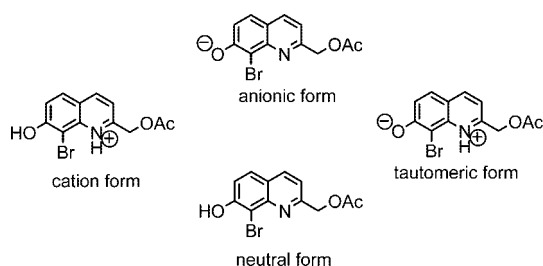
It is important to note that 8-bromo-7-hydroxyquinoline caged acetate (BHQ–OAc) is a derivative of 7-hydroxyquinoline (7-HQ), which has been extensively studied as a typical example having two prototropic functional groups of enol and imine in one molecule.^{8–18} Four prototropic species of 7-HQ are equili-

* To whom correspondence should be addressed. Tel: 852-2859-2160 (D.L.P.), 1-706-583-0423 (T.M.D.), FAX: 852-2957-1586 (D.L.P.), 1-706-542-9454 (T.M.D.), E-mail: phillips@hkucc.hku.hk (D.L.P.), tdore@chem.uga.edu (T.M.D.).

[†] The University of Hong Kong.

[‡] University of Georgia.

SCHEME 1



brated in aqueous solution: a normal molecule (7-HQ(N)), an imine-protonated cation (7-HQ(C)), an enol-deprotonated anion (7-HQ(A)), and an enol-deprotonated imine-protonated tautomer (7-HQ(T)).⁸ The pK_a of the phenolic moiety of 7-HQ has been reported to be 9.0.¹⁴ Equilibrium constants⁸ indicate the major species are the normal molecules (67%) and tautomers (29%) with minor species of cation (3%) and anion (1%) also present in water at pH 7. Several studies have focused on the ground singlet states and excited single and triplet states of 7-HQ and some derivatives.^{9,11–13} The mechanisms of the proton tautomerization of 7-hydroxyquinoline and the participation of solvent molecules have been explored in nonaqueous protic solvents^{8,10,11,14} and in aqueous solution.^{13,15–17} It is conceivable that BHQ–OAc, as a derivative of 7-HQ, may have similar properties but the influence of its substituent groups on these properties is not yet clear. The ground-state of BHQ–OAc is also a singlet electronic state.^{6,7} A cationic (quinolinium) form of BHQ–OAc(C), an anionic (quinolinate) form of BHQ–OAc(A), a neutral form of BHQ–OAc(N) are likely the major forms present in acidic, alkaline, and neutral aqueous solutions respectively, according to its acid–base equilibrium. In addition, a tautomeric form of BHQ–OAc(T) may also coexist with the neutral form in neutral aqueous solutions (Scheme 1). Nevertheless, the pK_a of the phenolic moiety in BHQ–OAc is 6.8,^{6,7} which is much lower than that of 9.0 for 7-HQ and might alter the ratios of the different forms existing in neutral aqueous solutions.

Because of the keen interest in the two-photon excitation and the desired applications of BHQ-protected carboxylates in biological experiments, it is necessary to clarify which species are the major ones in aqueous environments. This characterization of the ground-state species will provide the foundation for further detailed work on the photophysics and the photochemistry of BHQ–OAc. We report an absorption and resonance Raman spectroscopy study to elucidate and characterize the species of BHQ–OAc present in acetonitrile and mixed water/acetonitrile solutions at various pH values. To our knowledge, this is the first resonance Raman study conducted to characterize the ground-state forms of BHQ phototriggers. The absorption spectra of BHQ–OAc in water display no absorption bands of the tautomeric species in contrast to 7-HQ in aqueous solution, which displays a strong band at about 400 nm due to its tautomeric species. The BHQ–OAc resonance Raman spectra show a double Raman band system characteristic of the neutral form and a single Raman band diagnostic of the enol-deprotonated anion form and this indicates that the neutral form of BHQ–OAc is the major species in neutral aqueous solution. There is a modest increase in the amount of the anionic form and a substantial decrease in the amount of the tautomeric form of the molecules for BHQ–OAc compared to 7-HQ in neutral aqueous solution. The large substituent effect found for BHQ–OAc in neutral solution could be due to the steric and/or electronic effects of the 8-bromo group and/or competitive

hydrogen bonding between the 8-bromo group and water molecules that hinder the formation and transfer process of a BHQ–OAc–water cyclic complex.

Experimental and Computational Methods

8-Bromo-7-hydroxyquinoline caged acetate (BHQ–OAc) was prepared as described previously in the literature.⁶ Samples for the experiments described in this work were prepared using spectroscopic grade acetonitrile (MeCN) solvent and deionized water. NaOH and HClO₄ were used as needed to obtain sample solutions under acid/basic conditions.

A. Absorption and Resonance Raman Experiments. UV–vis spectra were recorded on a PerkinElmer Lambda 19 UV–vis spectrometer. Resonance Raman experiments were performed for BHQ–OAc in acetonitrile (MeCN) and NaOH–H₂O/MeCN (60:40 v/v, pH 11~12) and H₂O/MeCN (60:40 v/v, pH 6~7) mixed solvents. The concentrations were about 3 mM BHQ–OAc for the sample solutions. The experimental apparatus and methods used for these experiments have been described elsewhere¹⁹ and only a short description will be given here. The resonance Raman experiments were conducted using 266 nm excitation (fourth harmonic from a Nd:YAG laser) with about 0.9 mW laser power. The excitation laser beam was loosely focused to about a 0.5 mm diameter spot size onto a flowing liquid stream of sample. A back scattering geometry was employed for sample excitation and for collection of the Raman scattered light by reflective optics. The Raman signal detected by a liquid nitrogen cooled charge-coupled device (CCD) detector was acquired for 30 s before being read out to an interfaced personal computer and 10 of these readouts were added together to get the resonance Raman spectrum. The Raman bands of the MeCN solvent were employed to calibrate the resonance Raman spectra with an estimated accuracy of ± 5 cm⁻¹ in absolute frequency, and the solvent Raman bands were subtracted from the resonance Raman spectra using an appropriately scaled solvent spectrum.

B. Density Functional Theory (DFT) Calculations. The optimized geometry, vibrational modes, and vibrational frequencies for the singlet ground states of the neutral form, the anionic form, and the tautomeric form of BHQ–OAc were obtained from (U)B3LYP/6-311G** DFT calculations. No imaginary frequency modes were observed at any of the optimized structures shown here. A Lorentzian function with a 25 cm⁻¹ bandwidth was used with the computed Raman vibrational frequencies and their relative intensities to determine the (U)B3LYP/6-311G** calculated Raman spectra to compare with the corresponding experimental resonance Raman spectra. TD-DFT-RPA calculations were also performed for the species of interest to estimate their electronic transition energies and oscillator strengths as well as to predict the relevant frontier molecular orbitals related to the electronic transitions. All of the calculations were executed using the *Gaussian 03* program suite.²⁰

Result and Discussion

BHQ–OAc appears to exist as the normal neutral molecular form (BHQ–OAc(N)) in organic solvents that do not contain water. In aqueous solutions, the pK_a value of the phenolic moiety in BHQ–OAc is reported to be 6.8^{6,7} and thus BHQ–OAc exists almost exclusively in the anionic (hydroxylate) form at pH values larger than 8.8. At pH values near 7 in aqueous solutions, the BHQ–OAc neutral form is probably still one of the major species but other forms of BHQ–OAc are also likely to coexist in appreciable amounts. Therefore, we have done spectroscopic

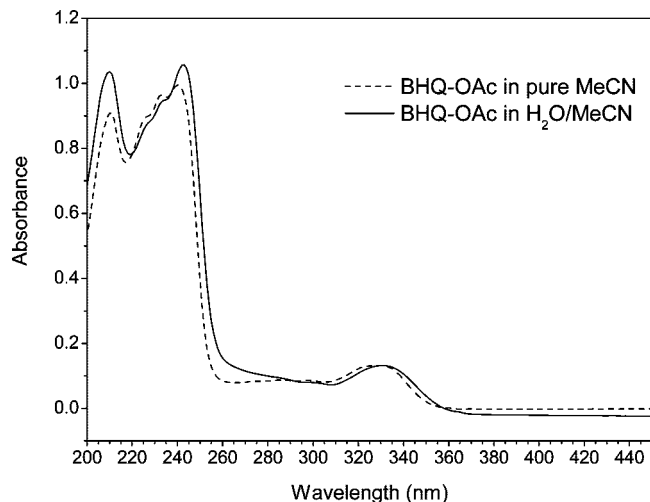


Figure 1. UV-vis absorption spectra of BHQ-OAc in acetonitrile and in H₂O/MeCN (60:40, v/v, pH 6~7) mixed solvents.

studies in H₂O/MeCN (60:40, v/v, pH 6~7), as well as in acetonitrile and in NaOH-H₂O/MeCN (60:40, v/v, pH 11~12), to obtain a better characterization of the forms of the ground-state species of BHQ-OAc in aqueous solutions.

A. Absorption Spectra in Acetonitrile and Mixed H₂O/MeCN Solvents. The lowest absorption bands of the different equilibrium forms of 7-HQ in aqueous solutions have been reported to be spectrally easy to distinguish.¹³ The 7-HQ(N), 7-HQ(C), 7-HQ(A), and 7-HQ(T) species can be differentiated by the position of their lowest energy absorption bands, which are at ~330, ~350, ~360, and ~400 nm respectively for the different forms of 7-HQ.¹³ Similarly, the UV-vis absorption spectra of BHQ-OAc existing in acetonitrile and H₂O/MeCN (60:40, v/v, pH 6~7) mixed solvents were measured (Figure 1). The absorption spectrum of BHQ-OAc(N) obtained in acetonitrile with a long-wavelength absorption maxima located at around 330 nm is quite similar to the absorption band previously reported for the neutral form of 7-HQ ($\lambda_{\text{max}} = 326$ nm) in nonaqueous solutions.^{13,14} However, the absorption bands of 7-HQ in water^{13,17,18} reveal dual absorption bands with maxima of 328 and 400 nm due to the lowest electronic transitions of the normal and the proton-translocated tautomeric species, respectively. The absorption spectrum of BHQ-OAc obtained in H₂O/MeCN (60:40, v/v, pH 6~7) only shows a small red-shift compared to the spectrum obtained in acetonitrile with no obvious absorption band appearing around 400 nm attributable to BHQ-OAc(T). This may be explained in part by BHQ-OAc(N) still being the predominant species in aqueous solution and in part by BHQ-OAc(T) likely not being a major form in aqueous solution.

UV-vis absorption spectra of BHQ-OAc in MeCN and H₂O/MeCN (60:40, v/v) mixed solvents with varying pH values were obtained (Figures 2 and 3). Figure 2 shows the UV absorption spectra of BHQ-OAc in acid, neutral, and alkaline acetonitrile solutions. The long-wavelength absorption maxima of the three spectra of BHQ-OAc(C), BHQ-OAc(N), and BHQ-OAc(A) are located at 320 (and 365), 330, and 373 nm, respectively.

The UV absorption spectra of BHQ-OAc in acid, neutral, and alkaline acetonitrile solution are shown in Figure 3. Comparing the spectra obtained in either the acid or the alkaline solutions in Figures 2 and 3, the long-wavelength absorption of BHQ-OAc(C) and BHQ-OAc(A) in acetonitrile solution are similar to those in aqueous solution. The absorption spectrum of BHQ-OAc(A), especially, is almost the same from 200 to

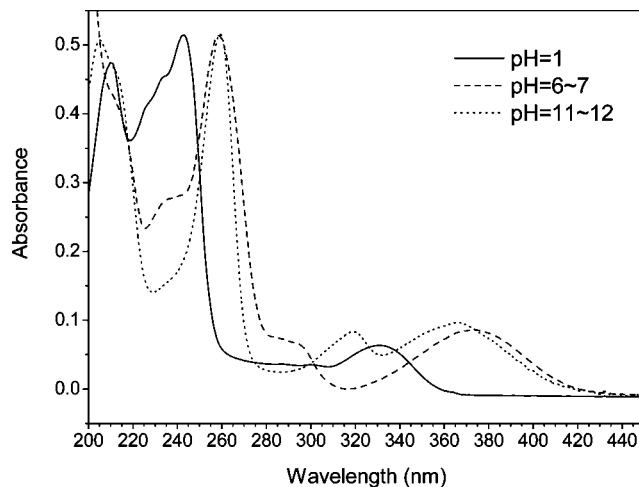


Figure 2. UV-vis spectra of BHQ-OAc in H₂O/MeCN (60:40, v/v) solvent at different pH values.

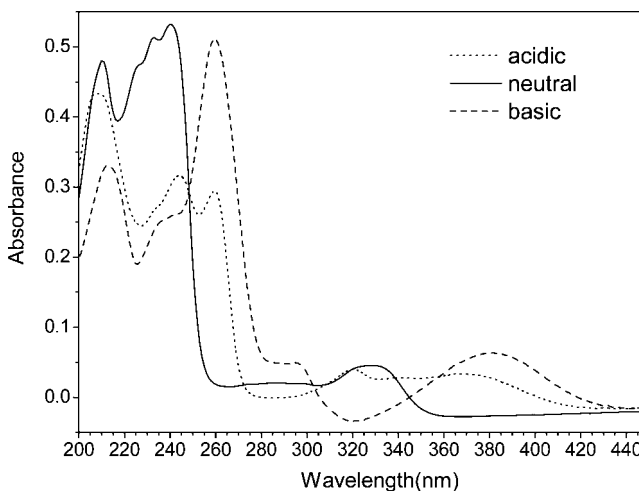


Figure 3. UV-vis spectra of BHQ-OAc in acetonitrile at different pH values.

450 nm regardless of solvent. It can be concluded that even in the presence of a small amount of basic solution in the acetonitrile system, the neutral form of BHQ-OAc can be transformed to the anionic form very easily.

A previously reported study indicated that only 3% 7-HQ(C) exists at pH 7 in the case of 7-HQ in water.⁸ Because the absorption spectra of BHQ-OAc shows no apparent broadening of the bands of BHQ-OAc(C), it may be likely that the BHQ-OAc(C) form are only present in a small amount in the neutral aqueous solution of BHQ-OAc, which is similar to the behavior of 7-HQ.⁸ In aqueous solutions of hydroxyquinolines,^{13,16} the UV absorption band contributed by the maxima of absorption of the tautomeric species usually appears at wavelengths that are longer than those for the anionic form (~400 nm). From a comparison of the spectra obtained in the neutral and alkaline aqueous solutions of BHQ-OAc, the maxima of BHQ-OAc(A) is located at 373 nm and there is no new obvious band appearing at wavelengths longer than 373 nm in neutral aqueous solutions that could be attributable to a tautomeric species. This suggests that the amount of the BHQ-OAc(T) species is very little in the aqueous system. The UV spectra of BHQ-OAc at pH 7.2 in a KMOPS buffer reported by Dore and co-workers^{6,7} shows the absorption of the phenolate ion ($\lambda_{\text{max}} \approx 370$ nm) and the phenol ($\lambda_{\text{max}} \approx 320$ nm). The former is located at about the same position as the maxima

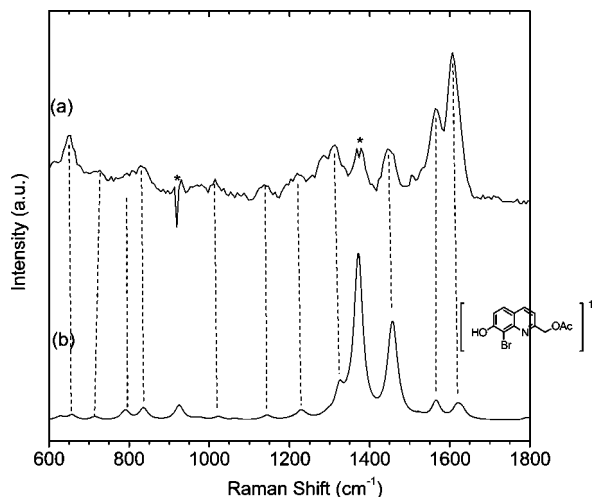


Figure 4. (a) 266 nm resonance Raman spectrum of BHQ–OAc obtained in acetonitrile. (b) (U)B3LYP/6-311G** calculated normal Raman spectrum of the singlet ground-state of the neutral form of BHQ–OAc, whose structure is shown to the right of the spectrum. The dashed lines indicate the correlation of the calculated Raman bands to the experimental resonance Raman bands. The asterisks (*) show the places of the solvent bands.

of BHQ–OAc(A) ($\lambda_{\max} = 373$ nm), so the absorption band at 370 nm in the neutral mixed aqueous solution is probably due to the absorption of BHQ–OAc(A). Compared to 7-HQ, BHQ–OAc(A) appears to modestly increase but BHQ–OAc(T) decreases substantially under the aqueous solvent conditions.

B. Resonance Raman Spectra of BHQ–OAc in Acetonitrile and in Neutral and Basic Mixed H₂O/MeCN Solvents. To further characterize BHQ–OAc(A) and/or BHQ–OAc(T) in the neutral aqueous solution coexisting with BHQ–OAc(N), resonance Raman spectra of BHQ–OAc in acetonitrile, in mixed NaOH–H₂O/MeCN solvent (60:40, v/v, pH 11~12), and in mixed H₂O/MeCN solvent (60:40, v/v, pH 6~7) were obtained.

Acetonitrile Solution. Figure 4 shows the resonance Raman spectrum of BHQ–OAc in acetonitrile. The experimental spectrum is compared to the normal Raman spectrum of BHQ–OAc(N) predicted from (U)B3LYP/6-311G** DFT calculations. Examination of Figure 4 reveals that there is good agreement between the resonance Raman spectrum and the calculated Raman spectrum of BHQ–OAc(N) for their vibrational frequency pattern with the calculated frequencies being within about 7 cm⁻¹ on average for the eleven experimental Raman bands. A comparison of the experimental and calculated vibrational frequencies, preliminary vibrational assignments, and qualitative descriptions of the vibrational modes in the 600 to 1800 cm⁻¹ region of Figure 4 is given in Table 1S of the Supporting Information. The experimental and calculated spectra in Figure 4 show some differences in their relative Raman intensity pattern, which can be accounted for by the experimental spectra being resonantly enhanced, whereas the calculated spectra are nonresonant Raman spectra. The resonance Raman spectrum and comparison to the predicted Raman spectrum in Figure 4 confirm the assignment of the predominant species in acetonitrile being the singlet ground-state of BHQ–OAc(N).

Alkaline Mixed Aqueous Solution. To learn more about the ground-state of BHQ–OAc(A) and whether it coexists in neutral aqueous solution, the resonance Raman of BHQ–OAc was obtained in mixed NaOH–H₂O/MeCN solvent (60:40, v/v, pH 11~12). Comparison of the two resonance Raman spectra obtained in acetonitrile and in the alkaline mixed aqueous solution (shown at the top of Figures 4 and 5, respectively)

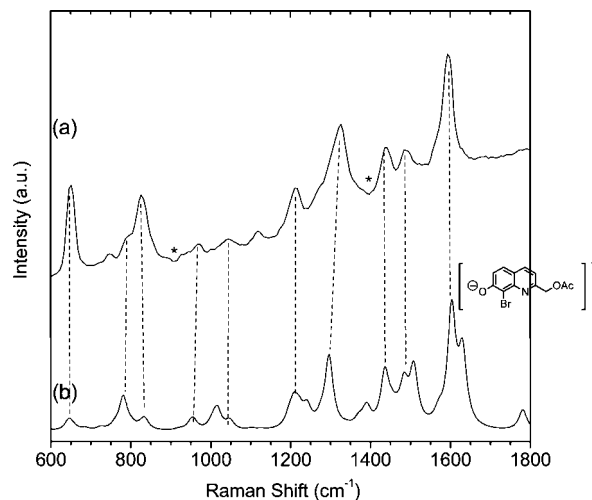


Figure 5. (a) 266 nm resonance Raman spectrum of BHQ–OAc obtained in mixed NaOH–H₂O/MeCN solvent (60:40, v/v, pH 11~12). (b) (U)B3LYP/6-311G** DFT calculated normal Raman spectrum of the singlet ground-state of the anionic form of BHQ–OAc, whose structure is shown to the right of the spectrum. The dashed lines indicate the correlation of the calculated Raman bands to the experimental resonance Raman bands. The asterisks (*) show the places of the solvent bands cause subtraction artifacts.

reveals that the double bands with the nominal C=C ring stretching, C–N stretching, and O–H bending modes at 1564 and 1607 cm⁻¹ in the resonance Raman spectrum of BHQ–OAc(N) are replaced by a single Raman band with the nominal C=C ring, C–N, and C–O⁻ stretching modes at 1593 cm⁻¹. This indicates that the structure and bonding of the species probed by the resonance Raman spectrum here change substantially compared to those of BHQ–OAc(N) observed in acetonitrile. Because it is conceivable that deprotonation of BHQ–OAc molecule will take place to form BHQ–OAc(A) in the basic mixed aqueous solution, the resonance Raman spectrum obtained in Figure 5 is compared with the normal Raman spectrum of BHQ–OAc(A) predicted from B3LYP/6-311G** DFT calculations. Inspection of Figure 5 shows good agreement between the resonance Raman spectrum and the calculated Raman spectrum for the singlet ground-state BHQ–OAc(A) vibrational frequency pattern with the calculated frequencies being within 8 cm⁻¹ on average for the 10 experimental Raman bands. A comparison of the experimental and calculated vibrational frequencies, preliminary vibrational assignments and qualitative descriptions of the vibrational modes in the 600 to 1800 cm⁻¹ region of Figure 5 is given in Table 2S of the Supporting Information. The experimental and calculated spectra in Figure 5 exhibit some differences in their relative Raman intensity pattern that can be explained by the experimental spectra being resonantly enhanced, whereas the calculated spectra are nonresonant Raman spectra. The resonance Raman spectra and comparisons to the predicted Raman spectra in Figure 5 confirm the assignment of the predominant species to the singlet ground-state of BHQ–OAc(A) in the mixed NaOH–H₂O/MeCN solvents (60:40, v/v, pH 11~12).

Neutral Mixed Aqueous Solution. The resonance Raman spectrum of BHQ–OAc measured in mixed H₂O/MeCN solvent (60:40, v/v, pH 6~7) is displayed at the top of Figure 6. We can see that the Raman bands appear much broader than those in the resonance Raman spectra obtained in the organic and alkaline aqueous solutions displayed at the top of Figures 4 and 5, respectively. The spectrum in the neutral mixed aqueous solution provides the overall Raman information of the different

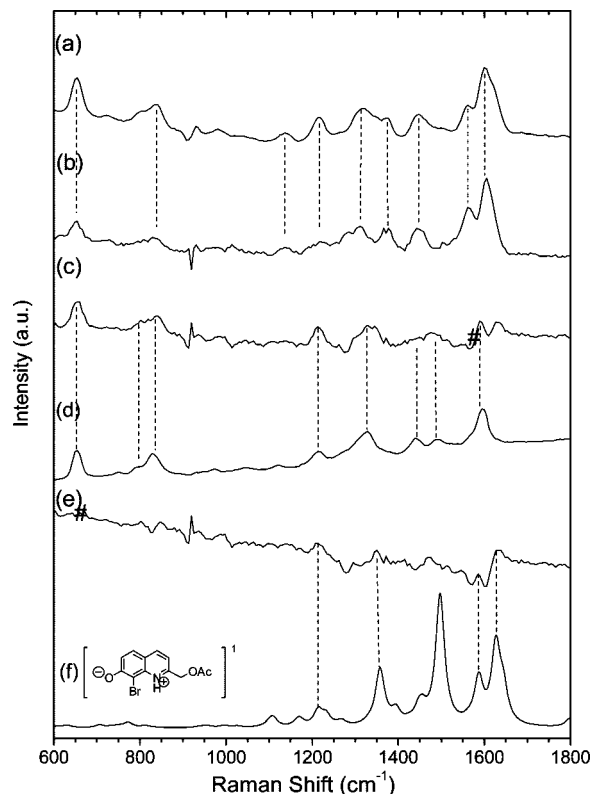


Figure 6. (a) 266 nm resonance Raman spectrum of BHQ-OAc obtained in mixed H₂O/MeCN solvents (60:40, v/v, pH 6~7). (b) 266 nm resonance Raman spectrum of BHQ-OAc obtained in acetonitrile. (c) The bands remaining after subtraction of an appropriately scaled (b) from (a). (d) 266 nm resonance Raman spectrum of BHQ-OAc obtained in mixed NaOH-H₂O/MeCN solvents (60:40, v/v, pH 11~12). (e) The bands remaining after subtraction of an appropriately scaled (d) from (c). (f) DFT calculated normal Raman spectrum of the singlet ground state of the tautomeric form of BHQ-OAc, whose structure is shown to the left of the spectrum. The dashed lines indicate the correlation of two spectra compared to each other. The pound signs (#) show the places where subtraction artifacts might be noticeable.

forms of BHQ-OAc in it. From both the investigation of the UV absorption spectra and the similar resonance Raman spectra obtained in acetonitrile and the neutral mixed aqueous solvent (parts a and b of Figure 6), it is reasonable to assume that BHQ-OAc(N) is still the major species in the neutral aqueous solution and contributes to the resonance Raman spectrum obtained in the neutral mixed aqueous solvent. The spectrum (c) in Figure 6 shows the bands remaining after subtraction of an appropriately scaled spectrum shown in part b of Figure 6 from the spectrum shown in part a of Figure 6. After subtraction, the medium bands existing in the resonance Raman spectrum of the neutral form of BHQ-OAc at 1564 and 1285 cm⁻¹ disappear. Then, comparing the spectrum after subtraction (part c of Figure 6) with the experimental resonance Raman spectrum of BHQ-OAc obtained in the basic mixed solvent (part d of Figure 6), the main bands in part d of Figure 6 at 1593, 1485, 1435, 1326, 1211, 827, 787, 651 cm⁻¹ are all included in part c of Figure 6. This suggests that the amount of BHQ-OAc(A) may increase modestly in the neutral aqueous solution. In addition, taking into account the UV-vis spectra in Figure 2, the strong bands of BHQ-OAc(A) obtained in the mixed solution can also be due to its strong absorption at 266 nm even though its concentration may be noticeably lower than BHQ-OAc(N). Similarly, part e of Figure 6 was obtained by subtracting an appropriately scaled spectrum of part d of Figure 6 from the spectrum shown in part c of Figure 6. The strong

bands in the spectrum of part d of Figure 6 at 1593, 1326, 827, and 651 cm⁻¹ assigned as BHQ-OAc(A) disappear, and the remaining bands at 1626, 1589, 1350, and 1213 cm⁻¹ have partial agreement with the normal Raman spectrum of the singlet ground state of the tautomeric form of BHQ-OAc predicted from the DFT calculations (part f of Figure 6). The double bands at 1589 and 1626 cm⁻¹ in the resonance Raman spectrum of BHQ-OAc(T) are described as the nominal C-C stretching, C-O⁻ stretching, and N-H bending modes in the calculation results (Table 3S in the Supporting Information). This suggests there may be a small amount of BHQ-OAc(T) in the solution since the resonance Raman spectrum of the tautomeric form of BHQ-OAc cannot be obtained directly because of the equilibrium between the BHQ-OAc(N) and BHQ-OAc(T) species and oversubtraction when obtaining the spectrum of BHQ-OAc(T) by subtracting the spectra of BHQ-OAc(N) and BHQ-OAc(A) (parts b and d of Figure 6) from the overall spectrum obtained in the neutral aqueous solution (part a of Figure 6).

Examination of the resonance Raman spectra in Figure 6 reveals that unlike 7-HQ in water at pH 7, the amount of BHQ-OAc(A) modestly increases in the neutral mixed aqueous solution. With the increase of BHQ-OAc(A), the number of molecules in the form of BHQ-OAc(T) decreases appreciably in the solution.

It is reasonable that the anionic form can be easily formed through the deprotonation of the phenol group of the neutral form in water environments. However, the formation of the tautomeric form is more complicated. Some previous studies showed that the participation of the solvent molecules plays an important role in the formation of the tautomeric species in both the excited and ground-state proton transfer reactions.⁹⁻¹⁸ The cyclic 7-HQ-solvent complex involving two solvent molecules was assumed as being precursors for the ground-state proton transfers (GSPT) to form the tautomeric molecules, and a more compact complex structure formed by two water molecules with 7-HQ may result in a higher probability of tautomerization.¹² This suggests that the ease of formation of the hydroxyquinoline-water complex could substantially affect the amount of the tautomeric form present in aqueous solutions. The appreciable decrease of the amount of BHQ-OAc(T) observed in the neutral mixed aqueous solution could mean that it is not favorable to form the cyclic BHQ-OAc-water complex here. This may be due to the presence of the 8-bromo group in several aspects. First, because of the presence of the bulky Br group, the steric hindrance introduced by the 8-bromo group might reduce the ability to form the complex species needed for tautomerization. This hypothesis is consistent with the observation of only small amounts of the complex of 8-methyl-7-hydroxyquinoline (8-Me-7-HQ) with two water molecules can be formed because of the hindrance of the 8-methyl group.¹⁴ Second, the inductively electron-withdrawing nature of bromine disfavors formation of a positively charged nitrogen. Third, because the Br atom can easily form hydrogen bonding with the water molecules in aqueous solutions, the competitive hydrogen bonding between the Br group and the water molecules also could make the cyclic complex hard to form. This explanation is consistent with the solvent rearrangement for 7-azaindole,²¹ which is necessary for its tautomerization but proceeds with difficulty in the ground or excited states in water because competitive hydrogen bonding yields a prevalence of the 7-azaindole polyhydrate species. Our experiments do not delineate which of these possibilities is the predominant reason for the different distribution of the ground-

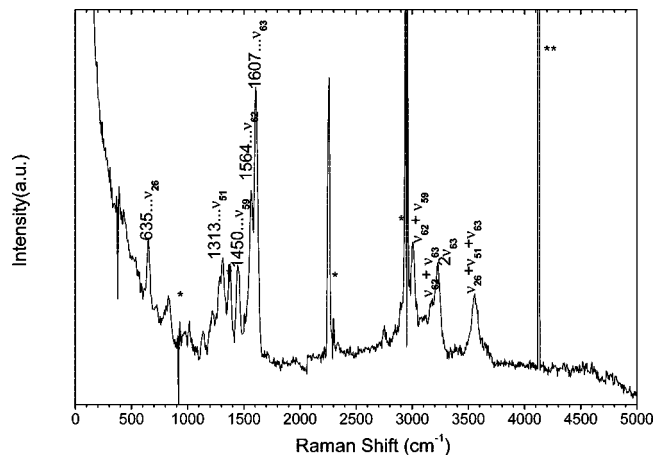


Figure 7. Resonance Raman spectrum of BHQ–OAc in acetonitrile solution obtained with 266 nm excitation (~ 3 mM concentration). The asterisks (*) mark solvent subtraction artifacts. The double asterisks (**) mark bands due to scattering from laser lines.

state forms of BHQ–OAc in neutral aqueous solution and they all may be operative to some degree.

The experimental resonance Raman spectra of the different forms of BHQ–OAc in aqueous solution also provide information about the electronic transition being excited and the Franck–Condon region dynamics in the excited state. We shall focus our discussion on the neutral and anionic forms of BHQ–OAc that can be directly obtained in acetonitrile and in the alkaline aqueous solution. Inspection of the experimental resonance Raman spectra shown in Figures 4–6 for the neutral and anionic forms of BHQ–OAc shows that the Raman intensity is partitioned into a number of vibrational modes that indicates the Franck–Condon region dynamics in the excited state have significant multidimensional character. At the 266 nm excitation wavelength, no clear feature was seen below 600 cm^{-1} in all of the resonance Raman spectra. The resonance Raman spectra obtained in both neutral and basic aqueous solutions appeared to have no obvious bands above 1800 cm^{-1} . However, several combination and overtones bands were observed in the high wavenumber region for the resonance Raman spectrum obtained in acetonitrile. A full spectrum covering the $0\text{--}5000\text{ cm}^{-1}$ region along with tentative assignments of the observed bands is presented in Figure 7. In addition to the fundamental Raman bands, the resonance Raman spectrum obtained in acetonitrile displays significant intensity in overtone progressions up to second order for the ring C=C and C \approx N stretching (ν) modes. This spectrum also displays intense combination bands between this mode and other resonance-enhanced modes (such as the ν_{62} , ν_{59} , and ν_{51} modes). The lack of or substantially lower intensity of similar overtones and combination bands in the spectra obtained in the aqueous solutions suggests that water may noticeably perturb the Franck–Condon region of the electronic excited state.

Time-dependent DFT calculations with the random phase approximation (RPA) were done to estimate the vertical transition energies, the oscillator strengths, and the changes in molecular orbitals involved in the electronic transitions. Table 1 shows the strongest oscillator strength transition obtained from TD-DFT calculations for the neutral and anionic forms of BHQ–OAc in the 225 to 275 nm region. The relevant frontier molecular orbitals related to the electronic transitions are displayed in the Supporting Information. According to the TD-DFT-RPA calculations (Table 1), the lowest unoccupied molecular orbital (LUMO) and the highest occupied molecular

TABLE 1: Electronic Transition Energies, Oscillator Strengths, and Related Molecular orbital Transitions for the Strongest Oscillator Strength Transition Obtained from (U)B3LYP/6-311G DFT Calculations for the Neutral and Anionic forms of BHQ–OAc in the 225 to 275 nm Region**

	neutral form	anionic form
excitation energy ^a	230.26 nm (0.5375)	261.56 nm (0.2790)
	74 \rightarrow 76 (0.47645)	72 \rightarrow 75 (0.38299)
	73 \rightarrow 76 (0.11294)	74 \rightarrow 80 (0.33869)
	73 \rightarrow 78 (–0.13453)	74 \rightarrow 79 (0.29858)
molecular orbital changes ^b	73 \rightarrow 75 (–0.25742)	69 \rightarrow 75 (0.13082)
	72 \rightarrow 77 (–0.11368)	74 \rightarrow 76 (–0.11587)
	70 \rightarrow 76 (–0.14970)	74 \rightarrow 77 (–0.19422)
	70 \rightarrow 75 (–0.22142)	

^a Numbers in parentheses are oscillator strengths of the corresponding excitations. ^b Numbers in parentheses are contributions of the configuration coefficients for the corresponding orbital changes to the excitations.

orbital (HOMO) of both neutral and anionic forms of BHQ–OAc are orbital 74 and 75, respectively. The excitation of the neutral form of BHQ–OAc is mainly formed from the transition of LUMO+1 \leftarrow HOMO with contributions of about 0.48. This excitation is predominantly a transformation of electron density from the π bonding orbital to the antibonding π^* LUMO+1 orbital. This excitation is mostly localized on the phenolic moiety, so it may accordingly be taken as a $\pi\pi^*$ state, consistent with the general assignment of the S_3 excited-state in similar systems.²² Such a change in the electronic configuration is expected to have a large oscillator strength as predicted by the RPA calculation. This transition results in a substantial weakening of the π ring system, which is consistent with the overtone and combinations of the ring 1607, 1564, and 1450 cm^{-1} C=C and C–N stretching modes observed in the resonance Raman spectrum obtained in acetonitrile. The excitation of the anionic form of BHQ–OAc has contributions from LUMO \leftarrow HOMO–2 with a configuration coefficient of 0.38, LUMO+5 \leftarrow HOMO with a configuration coefficient of 0.33, and LUMO+4 \leftarrow HOMO with a configuration coefficient of 0.29, leading to the promotion of ring bonding π electron to the antibonding π^* orbitals. The excitation of LUMO \leftarrow HOMO–2 involves the promotion of a large scale conjugated π system to the π^* LUMO orbital. From Table 1 and the results given in Figure 2S of the Supporting Information, it can be seen that almost all the relevant frontier molecular orbitals in the calculations of the neutral and anionic forms have little contribution from the acetate leaving group. This explains the absence of obvious resonance Raman bands related to the vibration of the acetate group in both of the resonance Raman spectra. It is interesting to note that the calculations for the anionic form show the LOMO+1 and LOMO+2 together with the LOMO and LOMO+3 frontier orbitals have noticeable contributions from the leaving group. This appears consistent with the hypothesis that the anionic form is the precursor of the photocleavage process as suggested in a previous experimental study.^{6,7}

Conclusions

The 8-bromo-7-hydroxyquinolinyl group (BHQ) is a derivative of 7-hydroxyquinoline (7-HQ). BHQ molecules coexist in different forms in aqueous solution and we employed absorption and resonance Raman spectroscopy to study the forms of the ground-state species of 8-bromo-7-hydroxyquinoline caged acetate (BHQ–OAc) in acetonitrile (MeCN), in $\text{H}_2\text{O}/\text{MeCN}$ (60:40, v/v, pH 6–7) and in $\text{NaOH}-\text{H}_2\text{O}/\text{MeCN}$ (60:40, v/v, pH 11–12). The absorption spectra of BHQ–OAc in water display

no discernible absorption bands of the tautomeric form in contrast to the strong band at about 400 nm observed for the tautomeric species of 7-HQ in aqueous solution. The resonance Raman spectra have two Raman bands (the nominal C=C ring stretching, C–N stretching, and O–H bending modes at 1564 and 1607 cm^{-1}) characteristic of the neutral form and a single Raman band (the nominal C=C ring, C–N, and C–O⁻ stretching modes in the 1593 cm^{-1} region) characteristic of the enol-deprotonated anionic form. This suggests that the neutral form of BHQ–OAc is the major species in neutral aqueous solution. For BHQ–OAc, there is a modest increase in the population of the anionic form and a large decrease in the population of the tautomeric form of the molecules compared to 7-HQ in neutral aqueous solution. This indicates that steric and/or electronic effects of the 8-bromo group and/or competitive hydrogen bonding between the 8-bromo group and water molecules hinders the formation of a cyclic BHQ–OAc–water complex, which could account for this large substituent effect.

Acknowledgment. This work was supported by a grant from the Research Grants Council of Hong Kong (HKU 7039/07P), the award of a Croucher Foundation Senior Research Fellowship (2006–07) from the Croucher Foundation and an Outstanding Researcher Award (2006) from the University of Hong Kong to D.L.P., an NSF CAREER Award (CHE-0349059) to T.M.D., and a summer fellowship from the UGA Graduate School to J.L.N.

Supporting Information Available: Tables of comparisons of the experimental resonance Raman spectrum vibrational frequencies and the density functional theory calculated vibrational frequencies over the 600 to 1800 cm^{-1} region along with preliminary vibrational assignments and qualitative descriptions of the vibrational modes for the singlet ground-state of the neutral form, the anionic form, and the tautomeric form of BHQ–OAc. Table displaying selected structural parameters determined for the ground states of the neutral form, the anionic form and the tautomeric form of BHQ–OAc from the (U)B3LYP/6-311G** calculations. Table showing selected electronic transition energies and oscillator strengths of the ground states of the neutral form, the anionic form, and the tautomeric form of BHQ–OAc obtained from the (U)B3LYP/6-311G** TD-DFT-RPA calculations. Table presenting Cartesian coordinates, total energies, and vibrational zero-point energies for the optimized geometry from the (U)B3LYP/6-311G** calculations for the ground states of the neutral form, the anionic form, and the tautomeric form of BHQ–OAc. Figure showing schematic diagrams for the structures obtained from the (U)B3LYP/6-311G** density functional theory calculations for the ground states of the neutral form, the anionic form, and the tautomeric form of BHQ–OAc. Figure showing a depiction of the HOMO and LUMO molecular orbitals for the strongest oscillator strength transition in the 225 to 275 nm region for the neutral form and the anionic form of BHQ–OAc. This material is available free of charge via the Internet at <http://pubs.acs.org>.

References and Notes

(1) (a) Givens, R. S.; Kueper, L. W. *Chem. Rev.* **1993**, *93*, 55–66. (b) Givens, R. S.; Goeldner, M. *Dynamic Studies in Biology: Phototriggers, Photoswitches and Caged Biomolecules*; Wiley-VCH: Weinheim, Germany, 2005.

- (2) Adams, S. R.; Tsien, R. Y. *Annu. Rev. Physiol.* **1993**, *55*, 755–784.
- (3) Dore, T. M. *Dynamic Studies in Biology: Phototriggers, Photoswitches and Caged Biomolecules*; Givens, R. S., Goeldner, M., Eds.; Wiley-VCH: Weinheim, Germany, 2005; pp 435–459.
- (4) (a) Denk, W.; Strickler, J. H.; Webb, W. W. *Science* **1990**, *248*, 73–76. (b) Denk, W. *Proc. Natl. Acad. Sci. U.S.A.* **1994**, *91*, 6629–6633.
- (5) (a) Furuta, T.; Wang, S. S. H.; Dantzker, J. L.; Dore, T. M.; Bybee, W. J.; Callaway, E. M.; Denk, W.; Tsien, R. Y. *Proc. Natl. Acad. Sci. U.S.A.* **1999**, *96*, 1193–1200. (b) Ando, H.; Furuta, T.; Tsien, R. Y.; Okamoto, H. *Nat. Genet.* **2001**, *28*, 317–325. (c) Lin, W. Y.; Lawrence, D. S. *J. Org. Chem.* **2002**, *67*, 2723–2726. (d) Montgomery, H. J.; Perdicakis, B.; Fishlock, D.; Lajoie, G. A.; Jervis, E.; Guillemette, J. G. *Biorg. Med. Chem.* **2002**, *10*, 1919–1927. (e) Lu, M.; Fedoryak, O. D.; Moister, B. R.; Dore, T. M. *Org. Lett.* **2003**, *5*, 2119–2122. (f) Suzuki, A. Z.; Watanabe, T.; Kawamoto, M.; Nishiyama, K.; Yamashita, H.; Ishii, M.; Iwamura, M.; Furuta, T. *Org. Lett.* **2003**, *5*, 4867–4870. (g) Furuta, T.; Takeuchi, H.; Isozaki, M.; Takahashi, Y.; Kanehara, M.; Sugimoto, M.; Watanabe, T.; Noguchi, K.; Dore, T. M.; Kurahashi, T.; Iwamura, M.; Tsien, R. Y. *ChemBioChem* **2004**, *5*, 1119–1128. (h) Goard, M.; Aakalu, G.; Fedoryak, O. D.; Quinonez, C.; St Julien, J.; Poteet, S. J.; Schuman, E. M.; Dore, T. M. *Chem. Biol.* **2005**, *12*, 685–693. (i) Perdicakis, B.; Montgomery, H. J.; Abbott, G. L.; Fishlock, D.; Lajoie, G. A.; Guillemette, J. G.; Jervis, E. *Biorg. Med. Chem.* **2005**, *13*, 47–57.
- (6) Fedoryak, O. D.; Dore, T. M. *Org. Lett.* **2002**, *4*, 3419–3422.
- (7) Zhu, Y.; Pavlos, C. M.; Toscano, J. P.; Dore, T. M. *J. Am. Chem. Soc.* **2006**, *128*, 4267–4276.
- (8) Mason, S. F.; Philp, J.; Smith, B. E. *J. Chem. Soc. A* **1968**, 3051–3056.
- (9) Thistlethwaite, P. J. *Chem. Phys. Lett.* **1983**, *96*, 509–512.
- (10) (a) Itoh, M.; Adachi, T.; Tokumura, K. *J. Am. Chem. Soc.* **1984**, *106*, 850–855. (b) Chou, P. T.; Wei, C. Y.; Wang, C. R. C.; Hung, F. T.; Chang, C. P. *J. Phys. Chem. A* **1999**, *103*, 1939–1949.
- (11) Konijnenberg, J.; Ekelmans, G. B.; Huizer, A. H.; Varma, C. *J. Chem. Soc., Faraday Trans. 2* **1989**, *85*, 39–51.
- (12) Bohra, A.; Lavin, A.; Collins, S. J. *Phys. Chem.* **1994**, *98*, 11424–11427.
- (13) Lee, S. I.; Jang, D. J. *J. Phys. Chem.* **1995**, *99*, 7537–7541.
- (14) Nakagawa, T.; Kohtani, S.; Itoh, M. *J. Am. Chem. Soc.* **1995**, *117*, 7952–7957.
- (15) Kim, T. G.; Kim, Y.; Jang, D. J. *J. Phys. Chem. A* **2001**, *105*, 4328–4332.
- (16) Poizat, O.; Bardez, E.; Buntinx, G.; Alain, V. *J. Phys. Chem. A* **2004**, *108*, 1873–1880.
- (17) Park, H. J.; Kwon, O. H.; Ah, C. S.; Jang, D. J. *J. Phys. Chem. B* **2005**, *109*, 3938–3943.
- (18) Kwon, O. H.; Kim, T. G.; Lee, Y. S.; Jang, D. J. *J. Phys. Chem. B* **2006**, *110*, 11997–12004.
- (19) (a) Li, Y. L.; Leung, K. H.; Phillips, D. L. *J. Phys. Chem. A* **2001**, *105*, 10621–10625. (b) Zhu, P. Z.; Ong, S. Y.; Chan, P. Y.; Leung, K. H.; Phillips, D. L. *J. Am. Chem. Soc.* **2001**, *123*, 2645–2649. (c) Zhu, P. Z.; Ong, S. Y.; Chan, P. Y.; Poon, Y. F.; Leung, K. H.; Phillips, D. L. *Chem.—Eur. J.* **2001**, *7*, 4928–4936. (d) Chan, P. Y.; Kwok, W. M.; Lam, S. K.; Chiu, P.; Phillips, D. L. *J. Am. Chem. Soc.* **2005**, *127*, 8246–8247. (e) Xue, J. D.; Guo, Z.; Chan, P. Y.; Chu, L. M.; But, T. Y. S.; Phillips, D. L. *J. Phys. Chem. A* **2007**, *111*, 1441–1451.
- (20) Frisch, M. J.; Trucks, G. W.; Schlegel, H. B.; Scuseria, G. E.; Robb, M. A.; Cheeseman, J. R.; Zakrzewski, V. G.; Montgomery, J. A. J.; Stratmann, R. E.; Burant, J. C.; Dapprich, S.; Millam, J. M.; Daniels, A. D.; Kudin, K. N.; Strain, M. C.; Farkas, O.; Tomasi, J.; Barone, V.; Cossi, M.; Cammi, R.; Mennucci, B.; Pomelli, C.; Adamo, C.; Clifford, S.; Ochterski, J.; Petersson, G. A.; Ayala, P. Y.; Cui, Q.; Morokuma, K.; Malick, D. K.; Rabuck, A. D.; Raghavachari, K.; Foresman, J. B.; Cioslowski, J.; Ortiz, J. V.; Baboul, A. G.; Stefanov, B. B.; Liu, G.; Liashenko, A.; Piskorz, P.; Komaromi, I.; Gomperts, R.; Martin, R. L.; Fox, D. J.; Keith, T.; Al-Laham, M. A.; Peng, C. Y.; Nanayakkara, A.; Gonzalez, C.; Challacombe, M.; Gill, P. M. W.; Johnson, B.; Chen, W.; Wong, M. W.; Andres, J. L.; Gonzalez, C.; Head-Gordon, M.; Replogle, E. S.; Pople, J. A.; *Gaussian 98*, rev., A.7 and *Gaussian 03* rev., B.05; Gaussian Inc., Pittsburgh PA: 1998, 2003.
- (21) Chou, P. T.; Martinez, M. L.; Cooper, W. C.; McMorro, D.; Collins, S. T.; Kasha, M. *J. Phys. Chem.* **1992**, *96*, 5203–5205.
- (22) (a) Dym, S.; Hochstra, Rm. *J. Chem. Phys.* **1969**, *51*, 2458–2468. (b) Silva, C. R.; Reilly, J. P. *J. Phys. Chem.* **1996**, *100*, 17111–17123. (c) Chan, W. S.; Ma, C. S.; Kwok, W. M.; Zuo, P.; Phillips, D. L. *J. Phys. Chem. A* **2004**, *108*, 4047–4058.

JP809586H